https://doi.org/10.1007/s10118-024-3208-3

Chinese J. Polvm. Sci.

Crosslinked Natural Rubber and Styrene Butadiene Rubber Blends/Carbon Black Composites for Self-healable and **Energy-saved Applications**

Ariya Julbusta, Kwanchai Buaksunteara, Supitta Suethaoa, Phillip Kohlc, Youli Lic, and Wirasak Smitthiponga, b*

- a Specialized Center of Rubber and Polymer Materials in Agriculture and Industry (RPM), Department of Materials Science, Faculty of Science, Kasetsart University, Chatuchak, Bangkok 10900, Thailand
- ^b Hub of Talents in Natural Rubber, National Research Council of Thailand (NRCT), Bangkok 10900, Thailand
- ^c Materials Research Laboratory, University of California, Santa Barbara, CA 93106, USA



Electronic Supplementary Information

Abstract Crosslinking natural rubber (NR) and styrene butadiene rubber (SBR) composites with carbon black (CB) have been utilized in the tire tread industry. A sulfur-based lightly crosslinker can potentially enhance the self-healing capabilities of rubber. Moreover, the rubber composites were studied for non-covalent interactions between the benzene rings of SBR and CB. In this research, rubber samples were prepared, and their structure was investigated using Fourier transform infrared (FTIR), and Raman spectroscopy. The red shift in Raman spectroscopy confirmed noncovalent interaction or hydrophobic interaction between SBR and CB in NR/SBR composites exposed to CB due to environmental change. The differential scanning calorimetry (DSC) thermograms showed that NR and SBR were incompatible. Additionally, the mechanical properties of these rubber blends were enhanced as the proportion of NR increased. The maximum self-healing performance reached 40% for the formulation containing 25 phr NR and 75 phr SBR, which also saved energy with low chain end movements. Therefore, these composites could be utilized as a semi-empirical model for studying crosslinked rubber blends, specifically in the rubber tire industry.

Keywords Crosslinked rubber; Natural rubber composites; Self-healing; Energy-saved application

Citation: Julbust, A.; Buaksuntear, K.; Suethao, S.; Kohl, P.; Li, Y. L.; Smitthipong, W. Crosslinked natural rubber and styrene butadiene rubber blends/carbon black composites for self-healable and energy-saved applications. Chinese J. Polym. Sci. https://doi.org/10.1007/s10118-024-3208-3

INTRODUCTION

Manufacturing energy-saving tire treads has generated considerable attention. Reducing the rolling resistance of tires could decrease energy consumption and fuel usage while reducing the emission of pollutants. Producing tires with low heat buildup poses another challenge, as the heat generated during dynamic cyclic loads promotes tire degradation.[1-3] Natural rubber (NR) is a sustainable material, scientifically known as Hevea brasiliensis. NR exhibits outstanding features, such as high molecular weight, and mechanical properties.[4-6] The utilization of NR, it is important to be cautious of the presence of fungi as it can have a negative impact on the rubber's quality. The elevated moisture content of the NR sheets promotes the proliferation of fungus. This issue is a significant challenge in NR manufacturing, since it has the potential to impact both the production circumstances and the quality of the end products. Hence, it is necessary to incorporate antifungal agents into the process

* Corresponding author, E-mail: fsciwssm@ku.ac.th Received April 20, 2024; Accepted July 23, 2024; Published online September 27, 2024

of NR synthesis. Most commercial antifungal medicines exhibit considerable toxicity and are not environmentally friendly. A review was conducted on the wood vinegars derived from various biomasses, including inner coconut shell, bamboo, and Eucalyptus woods. [7] Hence, NR has been utilized for various applications, especially in the automobile industry for tire treads.

Generally, rubber products must be blended and then crosslinked to attain the desired properties, especially mechanical properties.[8-10] Raw rubber is limited by weak mechanical properties and inconsistent physical characteristics. When blended with chemicals, such as accelerators, activators, crosslinking agents, and fillers, and subsequently vulcanized, the resulting vulcanizate possesses enhanced mechanical qualities.[11] The tire tread, responsible for gripping the road surface, is typically made of NR blended with SBR.[12,13] Silica is typically used as a filler in energy-saving tires. However, carbon black (CB) is a widely used conventional filler due to its low cost and compatibility with NR.[14-16]

Previous studies have investigated saving energy in the framework of rubber materials. In addition, the energy saving of rubber materials can be determined from the hysteresis, which is analyzed using the $tan\delta$ value (loss tangent). A lower tan δ suggests reduced hysteresis, resulting in minimal heat generation.^[17] The relationship between tan δ values at 0 and 60 °C relates to the wet grip and rolling resistance of the tire tread, respectively. A high tan δ value at 0 °C indicates excellent wet grip, while a high tan δ value at 60 °C indicates increased rolling resistance, requiring a greater amount of energy or fuel for motion.^[2,18–20]

Kim *et al.* conducted a study on SBR/organoclay nanocomposites utilizing *N,N*-dimethyldodecylamine and modified montmorillonite, [21] including studying the effects of using a metal stearate instead of stearic acid. The dynamic mechanical analysis study found that SBR with calcium stearate had better $\tan\delta$ values at 0 and 60 °C than formulations containing stearic acid due to the ion impact between the negatively charged silicate layer and the calcium cations.

Additionally, research has been performed to examine the $\tan\delta$ values associated with NR and SBR rubber blends for tires. Karabork *et al.* considered a 50/50 phr NR/SBR rubber blend, examining the differences between conventional and pyrolytic CBs and oils.^[22] They have found that rubber blends with a pyrolytic CB and pyrolytic oil had enhanced wet grip but increased hysteresis compared to those produced with conventional CB and oil. Typically, achieving both an extensive $\tan\delta$ at 0 °C and a minimum $\tan\delta$ at 60 °C simultaneously has been challenging. The wet grip performance from this work was low and requires further formulation development.

Furthermore, Xiao *et al.* studied a blend of NR and SBR that included ultrafine, fully vulcanized powder nitrile butadiene rubber (UFPNBR).^[23] This research examined a composite consisting of 20/80 phr of NR/SBR with CB. The tanô values at 0 and 60 °C were measured as 0.290 and 0.170, respectively. Subsequently, while adding UFPNBR to NR/SBR, the tanô value at 0 °C increased to 0.420, while the tanô value at 60 °C decreased to 0.155. Therefore, modifying NR/SBR with UFPNBR could increase the wet traction and reduce the rolling resistance of tires. Prior studies^[21–23] demonstrated favorable energy efficiency in rubber; nevertheless, it has been suggested that the self-healing efficiency could be hindered by higher crosslinking density.

Tire products that have incurred damage exhibit decreased mechanical properties, performance, and safety. Enhanced rubber with self-healing properties can reduce these concerns, extending the lifespan of the product. The self-healing capability of rubber products that have been crosslinked to form a 3D network structure is restricted when the rubber material is torn or damaged.[24] Self-repairing in composite rubbers has been studied. Boden et al. reported the competitive factors that result in the highest self-healing efficiency of sulfur-cured rubber.[25] A system cured with sulfur has dynamic crosslinking: the sulfur-free radical broken chain could be reconnected at a suitable temperature after the rubber was damaged. A low crosslinking density resulted in high molecular chain interdiffusion and provided a high self-healing performance. The maximum self-healing performance could be found in a medium crosslinking density with rubber chains that could diffuse and dynamic crosslinks that could reform bonds.[26,27]

Moreover, Hernández et al. investigated the self-healing properties of conventional vulcanized NR under heat and

pressure.^[28] The tensile strength of the rubber compound increased because the crosslinking density increased, while the maximum self-healing was reduced. This result showed effective chain interdiffusion occurred when the crosslinking density was low. The healing efficiency of the sample was about 80% after healing for around 7 h at 70 °C under a pressure of 1 bar. The free radical of a sulfur bridge was able to exchange and reform bonds, and polysulphanyl radicals were detected using electron spin resonance.

The SBR commonly used in the tire industry has an interesting benzene ring within its molecular composition. The benzene rings are expected to interact non-covalently with a benzene ring on the surface of the CB. The investigation of non-covalent interactions between the rubber matrix and fillers has been researched. Bahl *et al.* examined a new hybrid filler that reduces viscosity dispersion in SBR rubber compounds based on non-covalent interactions between lignin and CB. The phenyl propane unit of lignin forms a π - π interaction with CB,^[29] as confirmed through Raman spectroscopy and ¹H spin-lattice relaxation. Moreover, non-covalent interactions can also affect the self-healing capability of rubber.^[30] The filler distribution should promote self-healing performance, including reduction of heat build-up in samples because of the influence of non-covalent interactions.

Therefore, the present research differs from literature studies by focusing on self-healing a lightly crosslinked system and the energy-saving potential of NR/SBR rubber blends with CB composites. In addition, the non-covalent interactions between the benzene rings of the SBR and the CB were investigated. This new work demonstrates interesting features in the structure-properties relationship of polymer science, including good compromises between self-healing capabilities, wet grip, and energy savings of NR/SBR blended composites. This could be a semi-empirical model for utilization in tire treads in the automotive industry, we could reduce size and quantity of CB to reach the optimum mechanical properties without affecting self-healable and energy-saved applications.

EXPERIMENTAL

Materials

Natural rubber consisting of *cis*-1,4 polyisoprene (RSS1), solution styrene-butadiene rubber (SSBR), CB (N330), zinc oxide (ZnO), *N*-cyclohexyl-2-benzothiazole sulfenamide (CBS), steric acid and sulfur were supplied from Thai Sin Rubber Industry Co., Ltd., Samutsakorn, Thailand. The formulations were modified based on previous literature.^[28] However, this previous work focused on pure NR without a filler, while our work investigated the NR/SBR blend with CB filler. Table 1 presents the composite formulations used in the current research in phr (parts per hundred of rubber).

Preparation of Rubber Blends and Crosslinked Rubbers

NR and SBR were masticated to increase softness before adding the chemicals for 4 min at 30 °C using an internal mixer (MX-300, Chareon Tut) at 50 r/min of rotor speed in a 300 mL chamber volume with a fill factor of 0.8. Next, zinc oxide and steric acid were added. CB was added last for the composite formulation

Formulations (phr) Ingredients 100NR_CB 75NR_CB 50NR_CB 25NR_CB 100SBR CB NR 100 75 50 25 0 SBR 25 50 75 100 0 7nO 3 3 3 3 3 Stearic acid 1 1 1 1 1 0.14 0.14 0.14 0.14 CBS 0.14 Sulfur 0.7 0.7 0.7 0.7 0.7 CB 40 40 40 40 40

Table 1 The rubber blend composite formulations.

with filler and blended continuously for 3 min. The chemicals were blended well with the rubbers and mixing continued for 4 min. The rubber blend composites were also mixed in a two-roll mill (ML-D6L12, Chareon Tut), and CBS was added between the two rolls for 1 min. Then, sulfur was added and mixed for 9 min. The obtained rubber blend composites were equilibrated for 24 h before testing.

The crosslinking in the rubber composite was investigated by measuring the torque change over time with a moving die rheometer (MDR-01, CGM Technology) at a speed of 100 cpm (cycles per minute), an angle of 0.5°, and a curing temperature of 150 °C for 30 min. The rubber composites underwent vulcanization through a compression molding machine (PR1D-W300L350-PM-HMI, Chareon Tut) operating at 150 °C with different curing times.

Material Characterization

Small/wide angle X-ray scattering (SAXS/WAXS)

SAXS/WAXS measurements were performed on a high brightness SAXS/WAXS instrument custom-built by the BioPACIFIC MIP research team at the University of California, Santa Barbara (USA). This instrument utilizes a high brilliance liquid metal jet X-ray source (D2+ by Excillum) and a large hybrid photon counting detector (Eiger2 R 4M from Dectris). AgBe was used as a calibrant in the SAXS/WAXS experiments. For SAXS, we used a Qmax of 0.2 and a beam diameter of 0.8 nm. Qmax was changed to 2.5 for WAXS. SAXS and WAXS were each conducted for 15 min.

Attenuated total reflection-Fourier transform infrared (ATR-FTIR) spectroscopy

The important functional groups of the cured samples were investigated using ATR-FTIR (VERTEX 70, Bruker). The spectral region was 400–4000 cm⁻¹, and an average of 64 scans per sample was collected.

Raman spectroscopy

The cured samples examined using Raman spectroscopy (Xplo-RA Plus, Horiba), using a laser wavelength of 532 nm and 2 accumulations. The spectral region was 400–3200 cm⁻¹.

Bound rubber test

A 0.2 g of sample of uncured rubber was used to examine the rubber-filler interaction.^[31] The sample was soaked in 50 mL of toluene and then kept in a darkened place at equilibrium. After 24 h, the solvent was changed. After 7 days, the undissolved rubber was filtered and dried. The remaining rubber sample was weighed to calculate the percentage of bound rubber, as shown in Eq. (1):

Bound rubber (%) =
$$\frac{W_D}{W_O} \times 100\%$$
 (1)

where W_D is the precise weight of a dry uncured rubber after being soaked in toluene, and W_O is the initial weight of the undissolved rubber.

Moving die rheometer (MDR)

The curing time was determined by using MDR-01 (CGM Technology) at a speed of 100 cpm (cycle per minute), an angle 0.5 deg and a curing temperature at 150 °C for 30 min.

Rubber process analyzer (RPA)

The storage modulus (G') was investigated for the Payne effect. The RPA test was performed using a D-RPA 3000 (MonTech) at 60 °C, pre-heated for 1 min, a frequency of 1 Hz, and 200% strain.

Swelling test

A swelling test was used to characterize the crosslinking density of rubber networks. A cured specimen was immersed in toluene until it reached swelling equilibrium for 7 days. The swollen specimen was blotted to remove the solvent and weighed daily. The Flory–Rehner equation was used to investigate the crosslinking density per unit volume of rubber (v). [4,32]

Differential scanning calorimetry (DSC)

A differential scanning calorimeter (DSC 3+, Mettler-Toledo) was used to characterize the cured rubber samples. The DSC thermograms were recorded within the range of -80 °C to 60 °C, with a heating rate of 10 °C/min and under an N_2 atmosphere.

Electron spin resonance spectrometer (ESR)

ESR spectroscopy was performed using a spectrometer (Elexys 500, Bruker) equipped with a temperature controller (ER4131VT). The spectra were recorded at a frequency of 9.4 GHz, a modulation amplitude of 4 G, a microwave power of 2 mW, and temperatures of 70 and 80 °C.

Tensile test

The dumbbell-shaped sample had a test section of 5×20 mm and a grip section of 10×10 mm. The cured samples were tested using a tensile machine (Z005TN, Zwick/Roell).

Self-healing test

The press-cured sheet was cut into a dumbbell shape. The dumbbell-shaped sample had a test section of 5×20 mm and a grip section of 10×10 mm. The sample was cut in the middle with a clean blade and gently pressed together for 1 h at $80\,^{\circ}\text{C}$ under a pressure of 6.25 kg/cm² (0.61 MPa) in the compression molding machine. After 1 h, the samples were left at room temperature for at least 30 min before the self-healing performance of the original and healed samples was examined using the mechanical property determined by the tensile test.

Dynamic mechanical analysis (DMA)

Rectangles (1 \times 20 mm) of the cured samples were prepared for DMA analysis (DMA1, Mettler-Toledo). The test was performed in the extension mode using a temperature sweep from $-80\,^{\circ}\text{C}$ to $80\,^{\circ}\text{C}$ with a rate of 10 $^{\circ}\text{C/min}$, a frequency of 1 Hz, and a strain of 5 μ m. The samples were also subjected to the strain sweep test, performed from 1 μ m to 300 μ m at 100 $^{\circ}\text{C}$ and 1 Hz in extension mode.

RESULTS AND DISCUSSION

This study used five primary blended rubber formulations consisting of different proportions of NR and SBR, reinforced by the addition of CB and subsequent crosslinking. A lightly crosslinked system was prepared to investigate the self-healing properties, which could be utilized as a rubber tire tread. Furthermore, some tests, such as DSC analysis and FTIR and Raman spectroscopy, incorporated crosslinked pure NR and SBR samples.

Structure Characterization

Figs. 1(a) and 1(b) show the characteristic bands obtained from

ATR-FTIR spectroscopic analysis of the rubber samples. The characteristic bands of NR were associated with C—H stretching at 2959–2852 cm $^{-1}$, C=C stretching at 1660 cm $^{-1}$, C—H bending at 1446 and 1375 cm $^{-1}$, and C=C—H of $\it cis$ -1,4-polyisoprene at 837 cm $^{-1}$.[32] The characteristic peaks of SBR are associated with C—H stretching in aromatic rings at 3025 cm $^{-1}$, C=C stretching at 1661 cm $^{-1}$, C—H of CH $_2$ in aromatic rings at 1493 and 1450 cm $^{-1}$, and C—H out-of-plane bending in aromatic ring at 698 cm $^{-1}$.[33,34] The effect of both rubbers on various blends was also observed. The Raman spectra are presented in Figs. 1(c) and 1(d). The appearance of C—S stretching and S—S stretching bands at 594 and 462 cm $^{-1}$, respectively, confirms the curing of the NR.[28]

The SBR bands exhibited specific characteristics related to C—S and S—S stretching, observed at 621 and 459 cm⁻¹, respectively. [35] Fig. 1(d) shows CB within the samples. The experimental results indicated that NR 100 phr exhibited a Raman shift of the D-band at 1353 cm⁻¹. When the concentration of SBR increased, the D-band red shifted. These results indicate that the system was disrupted, and its surrounding en-

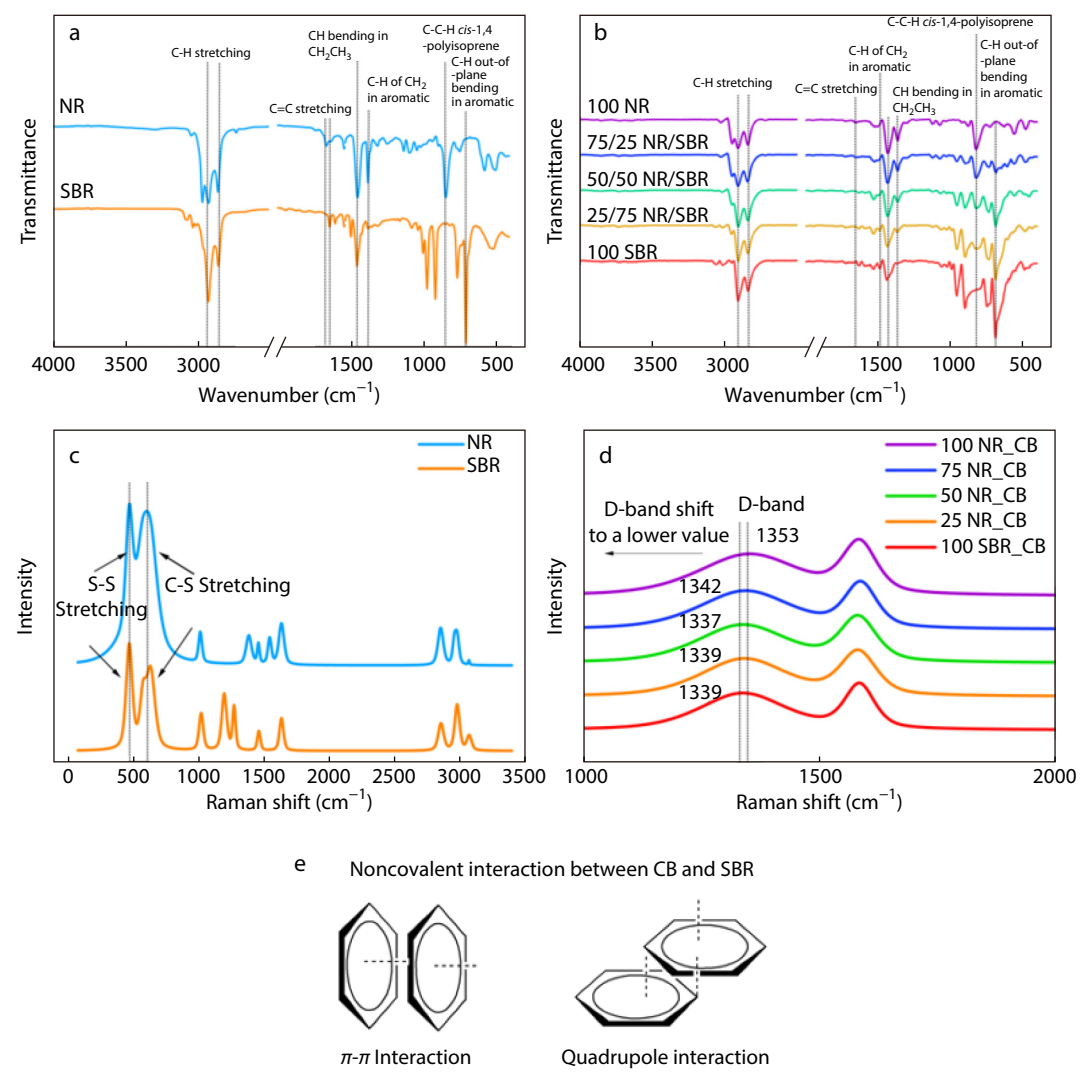


Fig. 1 ATR-FTIR spectra of samples (a) without CB and (b) with CB, and Raman spectra of rubber sample (c) without and (d) with CB, and (e) non-covalent interaction between CB and SBR.

vironment changed. It can be inferred that there is likely a non-covalent interaction or hydrophobic interaction between the benzene rings on the surface of the CB and the benzene rings of SBR.^[36] For the supplementary data, SAXS/WAXS information of the uncured and cured rubber samples are presented in Fig. S1 and Table S1 (in the electronic supplementary information, ESI).

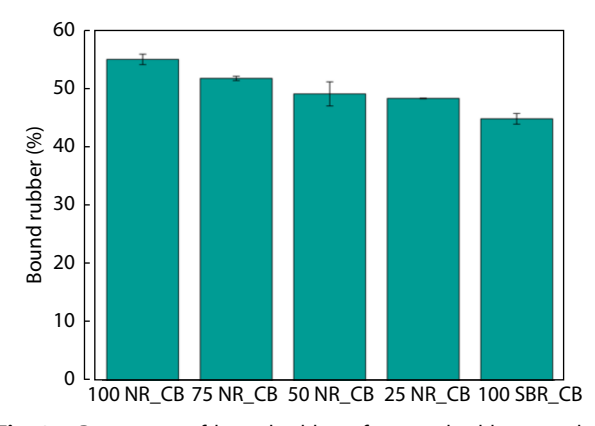
Rubber-filler Interaction

The filler-rubber matrix interaction was examined using the percentage of bound rubber, as shown in Fig. 2. The test results indicated that increasing the proportion of NR in the rubber blend sample resulted in a corresponding increase in the percentage of bound rubber. The longer molecular chains of NR enable it to exhibit superior CB adsorption capabilities than the shorter molecular chains of SBR. Normally, rubber with a higher molecular weight possesses a higher radius of gyration. [37] Table S1 shows that the radius of gyration of the NR was higher than that of the SBR. As a result, it can be assumed that NR had an increased probability of interacting with CB. [38]

Although Raman spectra studies indicate that SBR may participate in non-covalent interaction or hydrophobic interaction with CB, it is important to recognize that the number of chains in NR is higher than that of SBR. The hydrophobic interaction between the hydrocarbons of NR and CB may be more efficient, resulting in a larger amount of bound rubber in NR compared with SBR, with a difference of around 10%.

The CB can capture and distribute polymer radicals throughout its unique surface chemical structure. The ESR spectroscopy can be used to identify these types of delocalized radicals. Fang *et al.* provided a detailed description of the characteristics of ESR signals. A strong, narrow signal intensity suggests an enhanced interfacial interaction between NR and CB.^[39] The ESR spectra of samples cured at a healing temperature of 80 °C are shown in Fig. 3. Each spectrum demonstrated a consistent and distinct narrow signal with a G of 2.007. The NR with CB exhibited the strongest narrow signal intensity, and the signal declined as the amount of NR decreased. NR interacted better with CB than SBR, showing a trend consistent with previous bound rubber test results.

According to the results shown in Fig. 4(a), the crosslinked NR with CB had the highest curing curve. NR with 75 phr and 100 phr exhibite similar levels of high torque, showing that



 $\begin{tabular}{ll} \textbf{Fig. 2} & Percentage of bound rubber of uncured rubber samples \\ containing CB. \end{tabular}$

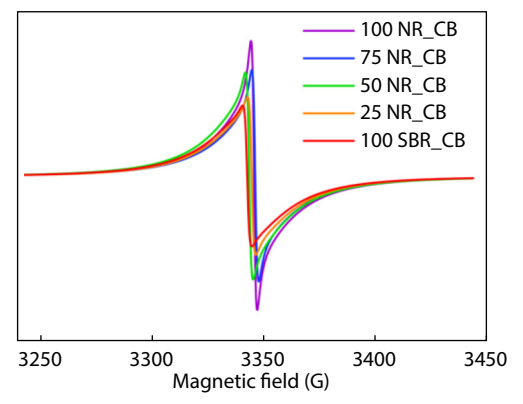
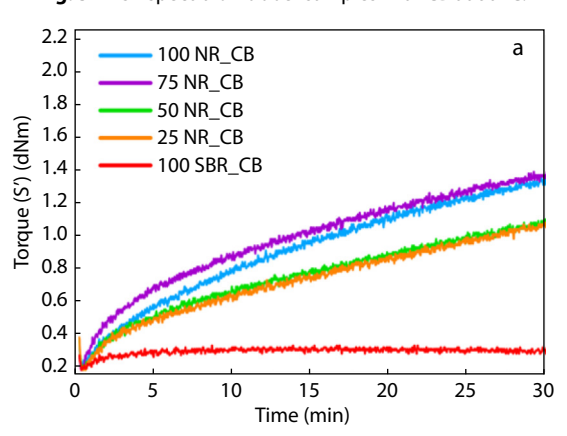


Fig. 3 ESR spectra of rubber samples with CB at 80 °C.



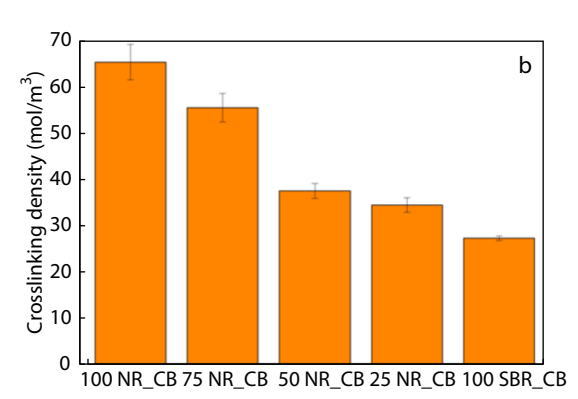


Fig. 4 (a) Rheometric curves of samples with CB at 150 $^{\circ}$ C and (b) crosslinking density of samples with CB.

the higher the torque value, the higher the crosslinking density. Moreover, the curing curve of NR at 25 phr was similar to that of NR at 50 phr.

Fig. 4(b) demonstrates the effect of the crosslinking density of the cured samples on swelling tests. The vulcanization process caused the molecular chains of rubber to create a three-dimensional network, enhancing its strength. The NR exhibited a greater degree of crosslinking density than the SBR. The maximum crosslinking density of 100 phr NR was approximately 65 mol/m³, whereas generally, the crosslinking density of NR reported in the literature review was about 100 mol/m³.^[4] This lower crosslinking density is due to the lightly crosslinking of this system. This study used around 1.3 g of sulfur (0.7 phr) and a minimal quantity of accelerator of 0.3 g

(0.14 phr). In contrast, the reference study used a significantly larger quantity of sulfur, 3 g, and 4 g of accelerator. Furthermore, the crosslinking density tended to decrease as the proportion of NR was reduced, which was consistent with the results of the curing curve.

Thermal Properties of Rubber Composites

In accordance with the DSC analysis of the rubber samples, Fig. 5 shows that the samples without CB had glass transition temperatures (T_g) of approximately $-65\,^{\circ}\mathrm{C}$ for NR and approximately $-34\,^{\circ}\mathrm{C}$ for SBR. This was in good agreement with the literature. [40,41] Including a small amount of sulfur did not discernibly impact the T_g . When the quantity of SBR in rubber blends increased, the T_g of the rubber blend increased. Due to the presence of long molecular chains in NR, the mobility of SBR is hindered, leading to a higher T_g . The sample blended with CB exhibited two T_g values, corresponding to the T_g values of NR and SBR. Thus, these blended rubbers were incompatible. The T_g values of all the samples are presented in Table S2 (in ESI).

Mechanical Properties and Hysteresis of Rubber Composites

The Payne effect was determined from the RPA of the rubber sample containing CB, as seen in Fig. 6. At low %strain, most of the filler remained agglomerated and formed a network, but at higher %strain, this filler network was destroyed, resulting in a decrease in the storage modulus of rubber (G').[20,42] When the difference in storage modulus (ΔG) between low and high %strain is not great, it suggests that the filler network is effectively disseminated. The results showed that NR had the lowest $\Delta G'$, which increased with the amount of SBR. NR possesses long molecular chains, which facilitate the more effective dispersion of CB compared with SBR. The $\Delta G'$ of samples is presented in the insert of Fig. 6(a). Interestingly, 100 phr SBR with CB has the lowest dissipation energy or $tan\delta$ (Fig. 6b). Generally, there are three sources of hysteresis: non-linearity (Payne effect) caused by the effects of the filler or the CB on rubber, [43] $T_{\alpha\prime}$ [44] and the chain ends of the rubber. [45] In this work, the low $tan\delta$ of SBR) did not support the Payne effect. We conducted the RPA experiment at 60 °C, unrelated to the $T_{\rm q}$ of NR or SBR. Thus, the key factor responsible for the minimum hysteresis of SBR should be the effect of chain ends, which will be verified in the next test.

The results of the tensile strength tests of cured rubber blends from 100 phr NR to 100 phr SBR at a healing temperature of 80 °C and a healing time of only 1 h with minimal pres-

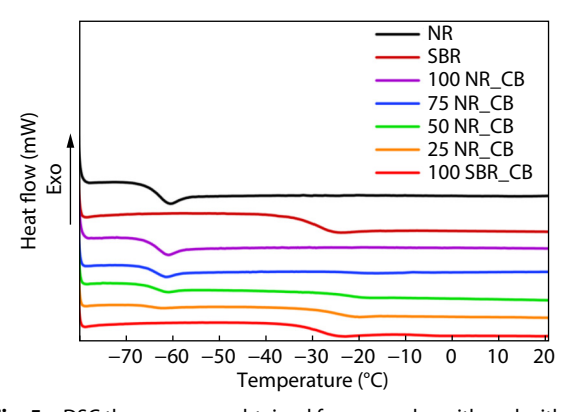


Fig. 5 DSC thermograms obtained from samples with and without CB.

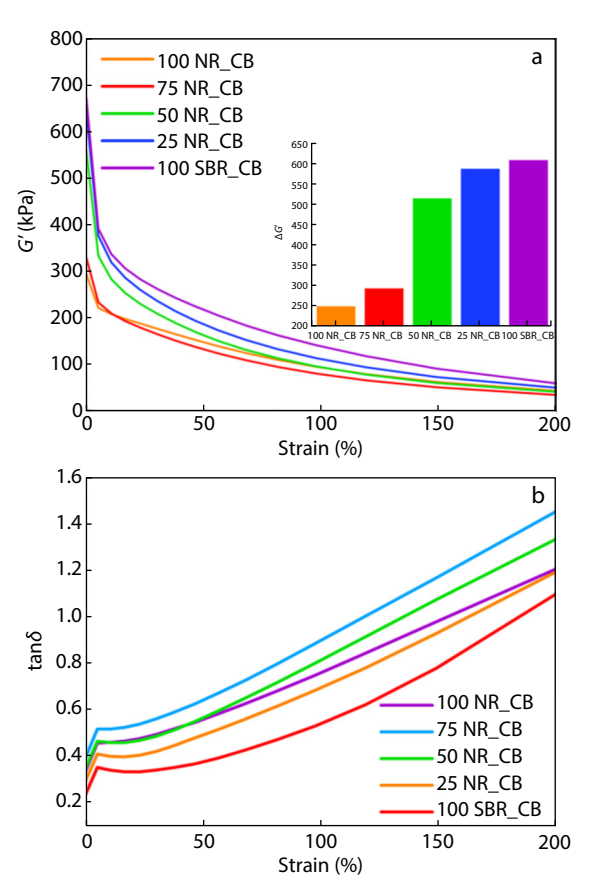


Fig. 6 RPA curves: (a) storage modulus (G') with $\Delta G'$ in the insert and (b) $\tan \delta$ of rubber samples containing CB.

sure are shown in Figs. 7(a)-7(e).

The tensile strength increased with larger amounts of NR. However, the elongation at break decreased after 50 phr of NR. We could reduce size and quantity of CB to reach the optimum mechanical properties requirements for tire treads without degrading self-healable and energy-saved applications. Figs. 7(a)–7(e) show a curve with solid lines representing the original samples and dashed lines representing self-healing samples. All data are summarized in Fig. 7(f). The initial image shows a sample that has been lightly crosslinked with CB, and subsequently cut apart. Then, the central image is subjected to a healable temperature of 80 °C and a healable pressure of 0.6 MPa. Finally, the interdiffusion of the free chain is expected to facilitate self-healing within one hour, as depicted in the last image. [46]

When the proportion of SBR increased, the self-healing performance tended to decrease due to the steric effect of the SBR molecules with benzene rings, causing poor chain interdiffusion between two pieces of rubber. The self-healing performance of samples with 25 and 50 phr of NR was within a narrow range of around 50%–60%, using a low pressure of 0.61 MPa (6.25 kg/cm²) at a healing temperature of 80 °C for 1 h (Fig. 7f). A study investigating the self-repairing capabilities of uncured epoxidized natural rubber (ENR), using metalligand interactions under a pressure of 1.03 MPa (150 psi) in a mold for 1 h at a healing temperature of 80 °C, has shown that the self-healing efficiency was approximately 60%. [47] Further-

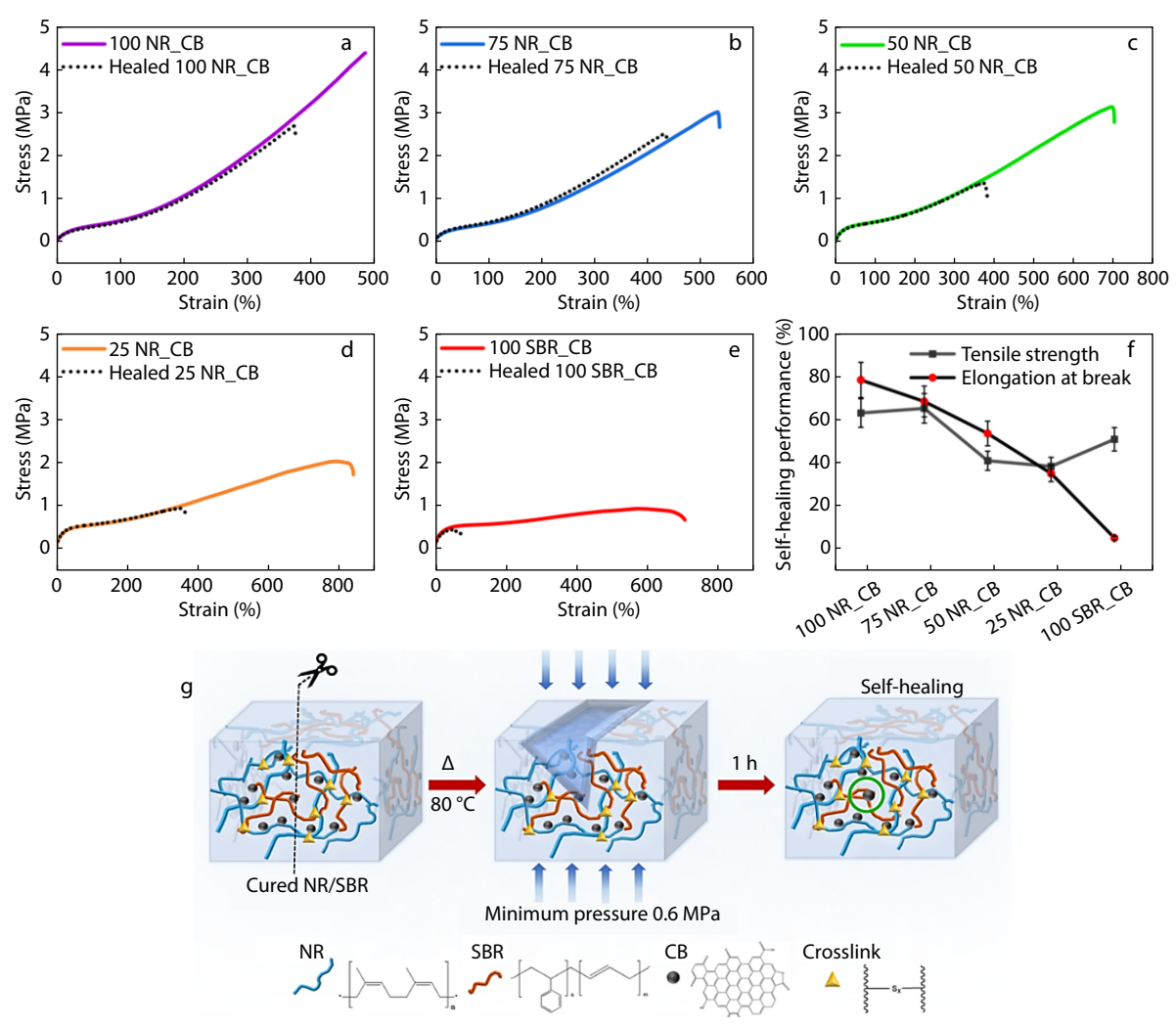


Fig. 7 (a—e) Self-healing results where the bold line refers to the original sample, the dashed line represents the self-healed sample, and (f) %self-healing performance on the tensile strength and elongation at break, and (g) the mechanism of the self-healing process.

more, using cured NR in the self-healing materials showed an efficacy of approximately 80% in enhancing the self-repairing capabilities of rubber that was healed at 70 °C and 1 bar (0.1 MPa) but required up to 7 h to heal. Additional research has also investigated the self-healing ability of NR composited with 40 phr of CB for different grades of CB. The maximum self-healing recovery of these NR/CB composites reached around 85% when using N660 of CB at a healing temperature of 80 °C, a healing period of 2 h, and a force of 2 N to improve the contact of the healing sample.

The self-healing test in this study used a pressure of 0.61 MPa (6.25 kg/cm²), and the material required a single hour for self-healing. The self-healing capability was around 40% for the rubber blends with 25 phr of NR and 75 phr of SBR. In the present study, the rubber blended with CB possessed good self-healing ability. The results may be slightly inferior to previous research that used ENR, NR, or NR/CB, likely due to the presence of an aromatic ring in SBR. [30,49]

Previous works studied only pure NR, long healing times, or high healing pressure. However, this study significantly impacted the self-healing of NR/SBR blends despite the shorter self-healing time and relatively low pressure. This NR/SBR rubber blend with CB composite could be applied in general tire treads.

Fig. 8(a) presents the DMA results of the rubber samples; the storage modulus (E') is displayed as a function of temperature. The transition regions of the NR and SBR samples differed. In rubber blends, increased SBR resulted in a separate transition region between NR and SBR, which was a dynamic glass transition temperature (T_q dynamic). The rubber blend samples had two tan δ peaks, which agree with the T_a dynamic of NR and SBR (Fig. 8b). This suggests that the blends were incompatible, in good agreement with the DSC results. The T_{q} dynamic of SBR was greater than that of NR, which aligns with the DSC investigation. In tire tread applications, the wet grip at 0 °C and rolling resistance at 60 °C are commonly evaluated factors, which can be analyzed using the tanδ.^[50,51] The rubber containing 25 phr of NR exhibited a high $tan\delta$ of 0.297 at 0 °C, indicating good wet grip for a tire tread compared with other formulations. It also demonstrated a low $tan\delta$ of 0.219 at 60 °C), suggesting optimal rolling resistance and potential fuel savings compared with the other formulations.

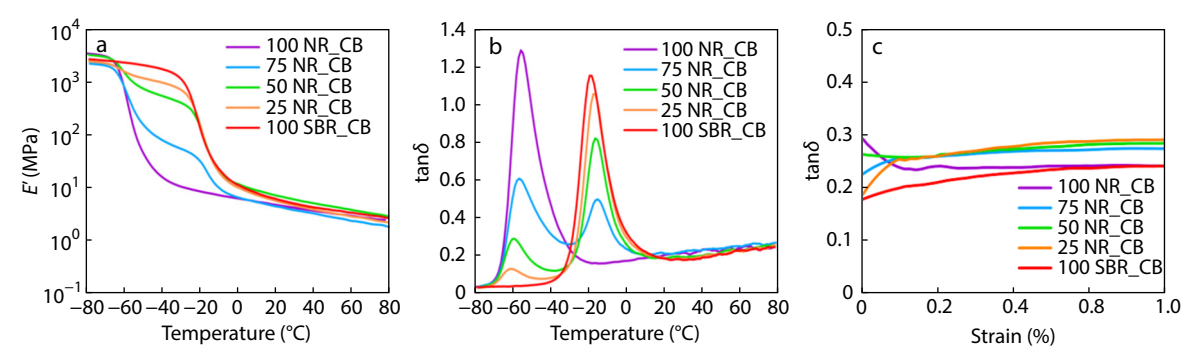


Fig. 8 DMA result of rubber samples with CB from temperature sweep test: (a) storage modulus (Ε'), (b) tanδ, and (c) tanδ from strain sweep test at temperature 100 °C.

The T_q dynamic of SBR significantly impacts its hysteresis at low temperatures, particularly at 0 °C. This greatly enhanced its resistance to wet skid: when considering 60 °C as the hysteresis of the tire rolling resistance, the SBR was lowest, according to Table S3 (in ESI).[2,18,19] When the composite containing 25 phr of NR and 75 phr of SBR with the reference data, it was found that this research exhibited a $tan\delta$ at 0 °C higher than the reference work, which used a 50/50 phr of NR/SBR with pyrolytic CB and pyrolytic oil,[21,22] and similar to previous work that used a 20/80 phr of NR/SBR with CB as a control sample.[23] The present research demonstrated that the traction on wet roads was exceptional. However, the $tan\delta$ at 60 °C in this study exceeded that of the reference data, which had a lower tanδ at 60 °C. This result could be attributed to a higher crosslinking density resulting from the use of higher concentrations of sulfur (1.75[22] and 1.90[23] phr) compared with this work, which only utilized 0.7 phr to produce a lightly crosslinked system. However, the present work achieved better self-healing efficiency than previous work due to the lightly crosslinked system.

Fig. 8(c) presents $tan\delta$ at 100 °C showing the hysteresis of rubber cha presents the $tan\delta$ at 100 °C, showing the hysteresis of the rubber chain ends. The effect of rubber chain ends in the sample is normally investigated at very low strain (<0.1%) and high temperature (100 °C).[52,53] We found that the $tan\delta$ or hysteresis of 100 phr of SBR and 25 phr of NR samples were similar at low $tan\delta$, indicating the effect of the rubber chain ends on the hysteresis of the composites. This result was in good agreement with the $tan\delta$ measured using RPA (Fig. 6b). Thus, the overall study indicated that the influence of the rubber chain ends performed an important role in determining the hysteresis of the composites in this work. Because SBR had a small number of chains compared with NR, it had the smallest chain end movements (lowest hysteresis). The 25 phr NR or 75 phr SBR composite is an interesting compromise new tire tread formulation in terms of self-healing, wet grip, and mechanical properties, while also providing energy efficient benefits.

CONCLUSIONS

In this work, NR and SBR were blended and also composited with CB. The samples used in this research include 100NR, 75NR/25SBR, 50NR/50SBR, 25NR/75SBR and 100SBR. These rubber samples were prepared to study lightly crosslinking and to

investigate the self-healing property of rubbers. The ATR-FTIR spectra confirmed important functional groups in the rubber samples, while Raman spectra showed a red shift in the D-band. The rubber blends containing CB showed considerably lower Dband Raman shift values. Thus, a non-covalent interaction or hydrophobic interaction exists between SBR and CB due to the changing environment. However, based on the result of the bound rubber analysis, rubber blends with a high NR content interacted with CB better than those containing SBR. ESR spectroscopy of rubber samples at a healing temperature of 80 °C showed that CB interacted better with the NR matrix, corresponding to the bound rubber analysis.

Moreover, rubber with a high NR content showed high maximum torque, which relates to high crosslinking density. For the thermal analysis of rubber samples, the DSC thermogram provided evidence of the incompatibility between NR and SBR. RPA analysis showed that NR dispersed CB more effectively than SBR. Regarding the self-healing properties of the rubber blends, 25 phr of NR was the compromise formulation, exhibiting a self-healing efficiency of 40%. The 25 phr of NR and 75 phr of SBR composite was highly effective in achieving optimal energy savings based on the $tan\delta$ obtained using DMA analysis.

The wet grip at 0 °C and rolling resistance at 60 °C are two regularly used evaluation variables in tire tread applications. The rubber containing 25 phr of NR and 75 phr of SBR represents a good compromise compared with other formulations. The $tan\delta$ from the strain sweep test conducted using DMA at 100 °C indicated that the main sources of hysteresis were the chain ends of the rubber. Therefore, this work established that the crosslinked rubber blends with CB have the potential to be beneficial as a material that can self-heal, has wet skid resistance, and saves energy as a new tire tread composite.

Conflict of Interests

The authors declare no interest conflict.



Electronic Supplementary Information

Electronic supplementary information (ESI) is available free of charge in the online version of this article at http://doi.org/ 10.1007/s10118-024-3208-3.

Data Availability Statement

The related data of this paper is data that should not be shared, and can be obtained from the author for reasonable reasons. The author's contact information: fsciwssm@ku.ac.th.

ACKNOWLEDGMENTS

The authors thankfully acknowledge the Graduate Scholarship, Faculty of Science, Kasetsart University. This work was supported by Budget Bureau, The Prime Minister's Office, Thailand (the strategic program on value creation agriculture for Kasetsart University in the fiscal year 2024), and supervised by Planning Division, Kasetsart University. The BioPACIFIC SAXS instrument was rendered with the support of the BioPACIFIC Materials Innovation Platform at UCSB, which is funded by the National Science Foundation (NSF) under Award No. DMR-1933487. Moreover, the authors also would like to acknowledge their gratitude to Asst. Prof. Dr. Soraya Pornsuwan from the Department of Chemistry at the Faculty of Science, Mahidol University, for providing crucial assistance with the electron spin resonance study.

REFERENCES

- Burlett, D. J. Thermal techniques to study complex elastomer/filler systems. J. Therm. Anal. Calorim. 2004, 75, 531–544.
- 2 Sae-oui, P.; Suchiva, K.; Thepsuwan, U.; Intiya, W.; Yodjun, P.; Sirisinha, C. Effects of blend ratio and SBR type on properties of silica-filled SBR/NR tire tread compounds. *Rubber Chem. Technol.* 2016. 89, 240–250.
- Wang, X.; Ji, Y.; Luo, Z.; Zhang, H.; Zhong, J.; Liang, J. Reducing dynamic heat build-up of styrene butadiene rubber/carbon black by filling aramid pulp coated with natural rubber latex. J. Appl. Polym. Sci. 2022, 139, e52651.
- 4 Chollakup, R.; Suwanruji, P.; Tantatherdtam, R.; Smitthipong, W. New approach on structure-property relationships of stabilized natural rubbers. J. Polym. Res. 2019, 26.
- 5 Suethao, S.; Ponloa, W.; Phongphanphanee, S.; Wong-Ekkabut, J.; Smitthipong, W. Current challenges in thermodynamic aspects of rubber foam. Sci. Rep. 2021, 11, 6097.
- 6 Li, Z. X.; Kong, Y. R.; Chen, X. F.; Huang, Y. J.; Lv, Y. D.; Li, G. X. High-temperature thermo-oxidative aging of vulcanized natural rubber nanocomposites: Evolution of microstructure and mechanical properties. *Chinese J. Polym. Sci.* **2023**, *41*, 1287–1297.
- 7 Baimark, Y.; Niamsa, N. Study on wood vinegars for use as coagulating and antifungal agents on the production of natural rubber sheets. *Biomass Bioenergy* **2009**, *33*, 994–998.
- 8 Dong, H.; Luo, Y.; Zhong, B.; Bai, J.; Jia, D. Effects of vulcanization accelerator functionalized graphene on the co-vulcanization kinetics and mechanical strength of NR/SBR blends. *Polym. Test.* **2020**, *81*, 106169.
- 9 Porobić, S. J.; Marković, G.; Ristić, I.; Samaržija-Jovanović, S.; Jovanović, V.; Budinski-Simendić, J.; Marinović-Cincović, M. Hybrid materials based on rubber blend nanocomposites. *Polym. Compos.* 2019, 40, 3056–3064.
- 10 Jong, L. Particle reinforced composites from acrylamide modified blend of styrene-butadiene and natural rubber. *Polym. Compos.* 2019, 40, 758–765.
- 11 Gawad, A. A.; Wims, D. T.; Jana, S. C.; Pugh, C.; Kulkarni, A. Crosslinking of SBR compounds for tire tread using

- benzocyclobutene chemistry. *Rubber Chem. Technol.* **2019**, *92*, 25–42.
- 12 Nihat Ali Isitman , E. L. L. F. M. M., Luxembourg (LU) ; Claude Charles Jacoby , Wasserbillig (LU) 2019, US 10,336,889 B2.
- 13 Surya, K. P.; Bhowmick, A. K. Mechanical properties of natural rubber and styrene-butadiene rubber nanocomposites with nanofillers having different dimensions and shapes at low filler loading. *Rubber Chem. Technol.* 2022, 95, 385–412.
- 14 Shi, R.; Ren, M.; Li, H.; Zhao, J.; Liu, S.; Li, Z.; Ren, J. Graphene supported Cu nanoparticles as catalysts for the synthesis of dimethyl carbonate: effect of carbon black intercalation. *Mol. Catal.* 2018, 445, 257–268.
- 15 Zatirostami, A. Carbon black/SnSe composite: a low-cost, high performance counter electrode for dye sensitized solar cells. *Thin* Solid Films 2021, 725, 138642.
- 16 Zhao, A.; Shi, X. Y.; Sun, S. H.; Zhang, H. M.; Zuo, M.; Song, Y. H.; Zheng, Q. Insights into the payne effect of carbon black filled styrene-butadiene rubber compounds. *Chinese J. Polym. Sci.* 2020, 39, 81–90.
- 17 Rifdi Rizuan, M. I.; Abdul Wahab, M. A.; Romli, A. Z. Effect of carbon black structures towards heat build-up measurements and its dynamic properties. *Adv. Mater. Res.* 2015, 1134, 131–137.
- 18 Mukhopadhyay, R.; Chakrabarty, D.; Prakasan, M. P.; Samui, B. K. Hysteresis characteristics of high modulus low shrinkage polyester tire yarn and cord. *Rubber Chem. Technol.* 2011, 84, 565–579.
- 19 Shen, J.; Wen, S.; Du, Y.; Li, N.; Zhang, L.; Yang, Y.; Liu, L. The network and properties of the NR/SBR vulcanizate modified by electron beam irradiation. *Radiat. Phys. Chem.* 2013, 92, 99–104.
- 20 Wang, Z. P.; Zhang, H.; Liu, Q.; Wang, S. J.; Yan, S. K. Effects of interface on the dynamic hysteresis loss and static mechanical properties of illite filled SBR composites. *Chinese J. Polym. Sci.* 2022, 40, 1493–1502.
- 21 Kim, W. S.; Lee, D. H.; Kim, I. J.; Son, M. J.; Kim, W.; Cho, S. G. SBR/organoclay nanocomposites for the application on tire tread compounds. *Macromol. Res.* 2009, 17, 776–784.
- 22 Karabork, F.; Tipirdamaz, S. T. Influence of pyrolytic carbon black and pyrolytic oil made from used tires on the curing and (dynamic) mechanical properties of natural rubber (NR)/styrenebutadiene rubber (SBR) blends. eXPRESS Polym. Lett. 2016, 10, 72–82.
- 23 Xiao, X.; Cui, Q.; Liu, J.; Wang, Q. Effect of elastomer nanoparticles on improving the wet skid resistance of SBR/NR composites. *Rubber Chem. Technol.* 2016, 89, 262–271.
- 24 Mandal, S.; Das, A.; Euchler, E.; Wiessner, S.; Heinrich, G.; Sawada, J.; Matsui, R.; Nagase, T.; Tada, T. Dynamic reversible networks and development of self-healing rubbers: a critical review. *Rubber Chem. Technol.* **2023**, *96*, 175–195.
- 25 Smitthipong, W.; Nardin, M.; Schultz, J.; Suchiva, K. Adhesion and self-adhesion of rubbers, crosslinked by electron beam irradiation. *Int. J. Adhes. Adhes.* **2007**, *27*, 352–357.
- 26 Boden, J.; Bowen, C. R.; Buchard, A.; Davidson, M. G.; Norris, C. Understanding the effects of cross-linking density on the self-healing performance of epoxidized natural rubber and natural rubber. ACS Omega 2022, 7, 15098–15105.
- 27 Wang, D.; Tang, Z.; Huang, R.; Duan, Y.; Wu, S.; Guo, B.; Zhang, L. Interface coupling in rubber/carbon black composites toward superior energy-saving capability enabled by aminofunctionalized polysulfide. *Chem. Mater.* 2023, 35, 764–772.
- 28 Hernández, M.; Grande, A. M.; Dierkes, W.; Bijleveld, J.; van der Zwaag, S.; García, S. J. Turning vulcanized natural rubber into a self-healing polymer: Effect of the disulfide/polysulfide ratio. ACS Sustainable Chem. Eng. 2016, 4, 5776–5784.
- 29 Bahl, K.; Miyoshi, T.; Jana, S. C. Hybrid fillers of lignin and carbon black for lowering of viscoelastic loss in rubber compounds.

- Polymer 2014, 55, 3825-3835.
- 30 Buaksuntear, K.; Limarun, P.; Suethao, S.; Smitthipong, W. Noncovalent interaction on the self-healing of mechanical properties in supramolecular polymers. *Int. J. Mol. Sci.* **2022**.
- 31 Chollakup, R.; Suethao, S.; Suwanruji, P.; Boonyarit, J.; Smitthipong, W. Mechanical properties and dissipation energy of carbon black/rubber composites. *Comp. Adv. Mat.* **2021**, *30*.
- 32 Prasopdee, T.; Shah, D. U.; Smitthipong, W. Approaches toward high resilience rubber foams: morphology-mechanics-thermodynamics relationships. *Macromol. Mater. Eng.* **2021**, *306*.
- 33 Zhang, J.; Chen, H.; Zhou, Y.; Ke, C.; Lu, H. Compatibility of waste rubber powder/polystyrene blends by the addition of styrene grafted styrene butadiene rubber copolymer: effect on morphology and properties. *Polym. Bull.* 2013, 70, 2829–2841.
- 34 Burgaz, E.; Gencoglu, O.; Goksuzoglu, M. Carbon black reinforced natural rubber/butadiene rubber and natural rubber/butadiene rubber/styrene-butadiene rubber composites: Part I: Rheological, mechanical and thermomechanical properties. *Res. Eng. Struct. Mater.* **2019**.
- 35 El-Bardan, A. A.; Khattab, S. N.; Belal, M. A.; Abboudy, S.; Kamoun, E. A.; Doma, A. S. Compatibilization of vulcanized SBR/NBR blends using *cis*-polybutadiene rubber: Influence of blend ratio on elastomer properties. *Eur. J. Eng. Res. Sci.* **2019**, *3*, 135–143.
- 36 Picheau, E.; Impellizzeri, A.; Rybkovskiy, D.; Bayle, M.; Mevellec, J. Y.; Hof, F.; Saadaoui, H.; Noe, L.; Torres Dias, A. C.; Duvail, J. L.; Monthioux, M.; Humbert, B.; Puech, P.; Ewels, C. P.; Penicaud, A. Intense Raman D band without disorder in flattened carbon nanotubes. *ACS Nano* **2021**, *15*, 596–603.
- 37 Rudin, A.; Choi, P., Practical aspects of molecular weight measurements. In *The Elements of Polymer Science & Engineering*, **2013**; pp. 89–148.
- 38 Wang, D.; Tang, Z.; Huang, R.; Duan, Y.; Wu, S.; Guo, B.; Zhang, L. Interface coupling in rubber/carbon black composites toward superior energy-saving capability enabled by aminofunctionalized polysulfide. *Chem. Mater.* **2022**, *35*, 764–772.
- 39 Fang, S.; Wu, S.; Huang, J.; Wang, D.; Tang, Z.; Guo, B.; Zhang, L. Notably improved dispersion of carbon black for high-performance natural rubber composites via triazolinedione click chemistry. *Ind. Eng. Chem. Res.* 2020, *59*, 21047–21057.
- 40 Goyanes, S.; Lopez, C. C.; Rubiolo, G. H.; Quasso, F.; Marzocca, A. J. Thermal properties in cured natural rubber/styrene butadiene rubber blends. Eur. Polym. J. 2008, 44, 1525–1534.
- 41 Lindemann, N.; Schawe, J. E. K.; Lacayo-Pineda, J. Kinetics of the glass transition of styrene-butadiene-rubber: Dielectric spectroscopy and fast differential scanning calorimetry. *J. Appl. Polym. Sci.* **2021**, *138*, 49769.
- 42 Li, Z.; Sun, H. B.; Li, C. Y.; Lu, Y. L.; Qiao, W.; Ning, N. Y.; Zhang, L. Q.;

- Tian, M. Dispersion and filler network structure of fibrillar silicates in elastomers. *Chinese J. Polym. Sci.* **2016**, *34*, 858–872.
- 43 Monti, M.; Giannini, L.; Tadiello, L.; Guerra, S.; Papagni, A.; Vaghi, L. Thermally activable bistetrazoles for elastomers crosslinking. *Polymers* 2022, 14.
- 44 Menczel, J. D.; Judovits, L.; Prime, R. B.; Bair, H. E.; Reading, M.; Swier, S., Differential Scanning Calorimetry (DSC). In *Therm. Anal. Polym.*, 2009; pp. 7–239.
- 45 Sun, L.; Wang, Y.; Li, Y.; Zhang, C. Study on a novel N-functionalized multilithium initiator and its application for preparing star-shaped N-functionalized styrene-butadiene rubber. J. Appl. Polym. Sci. 2008, 109, 820–824.
- 46 Smitthipong, W.; Nardin, M.; Schultz, J.; Nipithakul, T.; Suchiva, K. Study of tack properties of uncrosslinked natural rubber. J. Adhes. Sci. Technol. 2004, 18, 1449–1463.
- 47 Buaksuntear, K.; Panmanee, K.; Wongphul, K.; Lim-arun, P.; Jansinak, S.; Shah, D. U.; Smitthipong, W. Enhancing mechanical properties and stabilising the structure of epoxide natural rubber using non-covalent interactions: metal-ligand coordination and hydrogen bonding. *Polymer* **2024**, *291*.
- 48 Xia, T.; Wemyss, A. M.; Salehiyan, R.; Heeley, E. L.; Hu, X.; Tang, F.; Sun, Y.; Hughes, D. J.; McNally, T.; Wan, C. Effective and fast-screening route to evaluate dynamic elastomer-filler network reversibility for sustainable rubber composite design. ACS Sustainable Chem. Eng. 2023, 11, 17857–17869.
- 49 Li, Z. J.; Zhong, J.; Liu, M. C.; Rong, J. C.; Yang, K.; Zhou, J. Y.; Shen, L.; Gao, F.; He, H.-F. Investigation on self-healing property of epoxy resins based on disulfide dynamic links. *Chinese J. Polym. Sci.* 2020, 38, 932–940.
- 50 Xu, T.; Jia, Z.; Li, J.; Luo, Y.; Jia, D.; Peng, Z. Study on the dispersion of carbon black/silica in SBR/BR composites and its properties by adding epoxidized natural rubber as a compatilizer. *Polym. Compos.* **2016**, *39*, 377–385.
- 51 Jiang, W.; Gu, J. Nanocrystalline cellulose isolated from different renewable sources to fabricate natural rubber composites with outstanding mechanical properties. *Cellulose* 2020, 27, 5801–5813.
- 52 Song, S.; Yeom, G.; Kim, D.; Ryu, G.; Hwang, K.; Ahn, B.; Choi, H.; Paik, H. J.; Chung, S.; Kim, W. Effects of the diamine chain end functionalized liquid butadiene rubber as a processing aid on the properties of carbon-black-filled rubber compounds. *Polymers* **2022**, *14*.
- 53 Bijina, V.; Jandas, P. J.; Jose, J.; Muhammed Ajnas, N.; Abhitha, K. P.; John, H. Tuning the low rolling resistance, wet grip, and heat build-up properties of tyre tread formulations using carbon black/thermally exfoliated graphite hybrid fillers. J. Appl. Polym. Sci. 2022, 140.